LARGE-SCALE WIND-TUNNEL STUDIES OF SEVERAL VTOL TYPES

By Mark W. Kelly

Ames Research Center

INTRODUCTION

In recent years several full-scale wind-tunnel investigations of various VTOL airplane configurations have been made by the National Aeronautics and Space Administration. These investigations have ranged from concepts using helicopter-type rotor systems, intended generally for cruising speeds up to the order of 200 to 300 knots, to those using high-disk-loading fans or engines, intended for cruising at high subsonic or, ultimately, supersonic speeds.

Typical schematic arrangements of the three categories of VTOL aircraft to be discussed in this paper are shown in figure 1. They include: (1) those using lightly loaded helicopter-type rotors, (2) those using moderately loaded airplane-type propellers, and (3) those using highly loaded ducted fans or lifting engines. The aircraft are described in detail in references 1 to 3 and in a subsequent paper by Ralph L. Maki and David H. Hickey. The purpose of this paper is to summarize the main results and conclusions applicable to these three VTOL aircraft concepts and, in particular, to define those problem areas in which further research and development is required.

SYMBOLS

ΔL	lift due to fan
F_{F_o}	fan static thrust
ΔD_F	drag due to fan
ΔM_F	moment due to fan
R	fan radius
V_∞	free-steam velocity
A	rotor disk area

D_m	momentum drag
m_j	fan mass flow
F_j	fan gross thrust
v_j	jet velocity
θ	jet deflection angle
T	propeller thrust
q	dynamic pressure
$C_{L_{MAX}}$	maximum lift coefficient
α_w	local angle of attack of wing
V_s	slipstream velocity
C_D	drag coefficient
C_L	lift coefficient
δ_F	flap deflection
δ_w	wing tilt angle
γ	flight-path angle
S_B	blade area
q_∞	free-stream dynamic pressure
W	weight
L/D	lift-drag ratio
$\bar{C}_L$	blade section mean lift coefficient
ρ	density

L
1
4
1
2

V_T tip speed

V/nD advance ratio

η propulsive efficiency

$$\phi = \text{arc tan } \frac{V}{\pi nD}$$

L
1
4
1
2

DISCUSSION

VTOL Concepts Employing Helicopter-Type Rotor Systems

Two concepts of VTOL aircraft using lightly loaded helicopter-type rotors have been investigated: (1) the unloaded-rotor convertiplane, typified by the McDonnell XV-1 and (2) the tilting-rotor convertiplane, typified by the Bell XV-3. Both of these machines use rotors having hovering disk loadings of the order of 5 to 7 pounds per square foot, which result in relatively low slipstream velocities in hover, of the order of 20 to 30 knots.

The power-weight ratio as a function of flight velocity for the XV-1 unloaded-rotor convertiplane is shown in figure 2 for both autogyro flight at high rotor speed and unloaded-rotor flight at low rotor speed. For comparison, power-weight ratio for the airplane with the rotor removed is also shown. These data indicate what is believed to be a fundamental limitation to the performance of this type of machine, namely, the high profile drag associated with the unloaded rotor. For this particular airplane the drag of the rotor blades and hub accounted for 45 percent of the total drag of the machine in airplane flight. The drag of the rotor could be decreased by further reducing rotor speed; however, this reduction in rotor speed will tend to increase rotor-blade flapping problems. On future designs this rotor drag could perhaps be reduced, but it is believed that it will always represent a significant percentage of the total airplane drag.

A similar plot of power-weight ratio as a function of flight speed for the XV-3 tilting-rotor convertiplane in both helicopter configuration and airplane configuration, with high and low rotor speed, is shown in figure 3. It should be noted that the power shown here is shaft power and includes the rotor efficiency. If the rotor speed in airplane flight is the same as that used for helicopter flight, the increment in flight speed obtained by conversion from helicopter to airplane configuration is only about 10 knots and is largely due to a reduction in propulsive efficiency of the rotor due to the low thrust required in airplane flight compared with that in helicopter flight. In order to avoid this loss in propulsive efficiency the XV-3 employs a gear shift to reduce rotor speed for cruise. This lower rotor speed enables the rotor blade elements to operate at high pitch closer to maximum L/D and results in propulsive efficiencies of the order of 80 percent. Even so, the maximum speed of the airplane is limited to approximately 125 knots. This limitation is due both to low installed power and to high profile drag. This high profile drag is not, of course, fundamentally involved in the tilting-rotor concept and could be reduced substantially on future designs. The effect of such a drag reduction on the XV-3 is shown in figure 4, which presents propulsive power available and propulsive power required for the existing XV-3 and for the airplane with the profile drag reduced by 50 percent. At the higher speeds there is a reduction in the power available due to a reduction in propulsive efficiency with increasing advance ratio for constant power coefficient. This reduction in propulsive efficiency could be alleviated by a further decrease in rotor speed. However, in the case of the teetering rotor used on the XV-3, such a reduction in rotor speed results in an increase in rotor blade flapping. As discussed in a subsequent paper by Hervey C. Quigley and David C. Koenig, this rotor flapping can lead to undesirable effects on airplane dynamic stability. This flapping problem can possibly be alleviated by mechanical means, such as pitch-flap coupling (δ_3), and it is believed that further research on this subject is definitely worthwhile.

It should be noted at this point that this necessity to operate the rotor at high advance ratios and high power coefficients to obtain high values of propulsive efficiency is not peculiar to low-disk-loading rotors such as that on the XV-3. The reason for this is that, regardless of disk loading, propellers having sufficient blade area to provide static thrust equal to aircraft weight in hovering flight will have too much blade area for efficient operation at the reduced thrust levels required during cruise, unless they are operated at high advance ratios. It is emphasized that this is true regardless of disk loading. The preceding statements are illustrated in figure 5, which shows the variation of propeller blade-loading coefficient with advance ratio required for optimum propulsive efficiency. Propeller blade-loading coefficient is defined here as propeller thrust per square foot of blade area divided by the free-stream dynamic pressure. For typical propellers, operation in or near the shaded area will result in propulsive efficiencies of the order of 80 percent or more over the range of advance ratios shown. A representative data point for the XV-3 rotor propeller at high rotor speed indicates the order of efficiency obtained when the propeller is operated far from the shaded area, in this case 60 percent. Also shown is a data point for the XV-3 rotor propeller at low rotor speed, which verifies that operation near the shaded area results in efficiencies of about 80 percent. From the equation shown in the upper right-hand corner of figure 5, it is seen that, for all VTOL propellers, the blade-loading coefficient during cruise is equal to the blade loading in hover W/S_B divided by the product of airplane lift-drag ratio and free-stream dynamic pressure. This equation is obtained from the conditions that thrust equals drag and lift equals weight for level unaccelerated flight. From this equation it is seen that VTOL configurations having high lift-drag ratios and high cruise speeds will tend to low values of blade-loading coefficient and thus to high advance ratios for optimum propulsive efficiency. By noting that the blade-loading coefficient during cruise is the hovering blade loading W/S_B divided by the product of airplane lift-drag ratio and cruising dynamic pressure, it is seen that two methods of raising the blade-loading coefficient to a higher level exist: (1) the dynamic pressure for a given cruise velocity can be reduced by cruising at altitude, and (2) the hover blade loading can be increased. However, as shown in the lower equation in figure 5, the hover blade loading is determined by the blade-section mean lift coefficient and tip speed used in hovering flight. Thus, there is a limit to the value of blade loading that can be obtained if blade stall and compressibility losses are to be avoided. The use of variable-camber propellers to obtain high values of mean lift coefficient appears to be one promising way of obtaining the desired increase in hover blade loading.

This discussion has shown that propellers having sufficient blade area to provide thrust equal to weight in hover will have too much blade area for efficient operation at the low thrust levels required in cruise, unless they are operated at high advance ratios, regardless of disk loading. One favorable aspect of high-advance-ratio operation is that the blade twist required diminishes as the advance ratio is increased, which is in the direction to more nearly match the relatively low twist required for optimum hovering efficiency. For rotor propellers having blades free to flap, the magnitude of blade flapping will generally increase with increasing advance ratio, unless special measures are taken to avoid this effect.

VTOL Concepts Using Moderately Loaded

Airplane-Type Propellers

Two types of VTOL aircraft using moderately loaded airplane-type propellers are considered; namely, the deflected slipstream and the tilt-wing—deflected-slipstream configurations. One important requirement for these aircraft is that the slipstream velocity must be high enough to keep the local wing angle of attack below that for wing stall. The ratio of propeller disk loading to free-stream dynamic pressure required to keep the local wing angle of attack below 15° is shown in figure 6 as a function of free-stream angle of attack. As noted in this figure, the ratio of disk loading to free-stream dynamic pressure is a function of the ratio of slipstream velocity to free-stream velocity. The boundary curve shown was computed from rotor momentum theory with the condition that the local wing angle of attack indicated in the velocity triangle should not exceed 15°. The ratio of disk loading to dynamic pressure can be increased basically in three ways: (1) by increasing propeller disk loading, (2) by decreasing wing loading, and (3) by increasing wing lift coefficient by the use of high-lift devices. Inasmuch as propeller disk loading directly affects hovering performance, whereas wing loading affects cruise performance, a careful study of these conflicting requirements must be made to obtain the best compromise.

The problem of wing stall is accentuated in descending or decelerating flight. Therefore, it is important that the selection of disk loading, wing loading, and high-lift devices be made to ensure that the desired angles of descent can be attained without encountering wing stall. The importance of wing stall is indicated in figure 7. On the left of this figure is shown lift coefficient as a function of net drag coefficient for the Ryan VZ-3RY deflected-slipstream airplane. The vertical axis $\left(C_D = 0\right)$ represents a condition of steady level flight, whereas the sloping lines represent the conditions for angles of descent of 10° and 20°. For the ratio of disk loading to dynamic pressure shown, it is seen that steady level flight can be maintained with some margin on wing stall, whereas an angle of descent of 10° requires flight very near wing stall, and an angle of descent of 20° requires flight beyond wing stall.

On the right-hand side of figure 7 are presented similar data obtained from full-scale wind-tunnel tests of a deflected-slipstream—tilt-wing airplane. As shown in the sketch in the lower right-hand corner of the figure, this configuration utilized both leading- and trailing-edge flaps. The trailing-edge flaps were equipped with boundary-layer control to increase their effectiveness. With these high-lift devices and with the relatively high ratio of disk loading to wing loading of this configuration, higher descent angles were expected than were experimentally obtained. The reason for this result apparently was that a large area of flow separation was encountered on the center section of the wing which spanned the fuselage and was not in the propeller slipstream. This flow separation not only limited maximum lift but also resulted in severe buffet. With regard to this buffeting it should be noted that these data were obtained at free-stream velocities which corresponded to wing loadings of about 20 pounds per square foot. On larger aircraft with higher wing loadings and flying at correspondingly higher speeds, it is anticipated that this buffeting would be very objectionable. These results indicate the importance of minimizing flow separation on portions of the wing outside of the propeller slipstream. Two possible approaches to alleviating this problem are (1) eliminate the flow separation by using more powerful stall control devices or lower wing tilt angles, and (2) minimize the area of the wing outside of the propeller slipstream.

Ducted Fans

Two general types of VTOL aircraft using ducted fans have been investigated, namely, those with fixed ducts such as the fan-in-wing or fan-in-fuselage designs, and those having tilting ducts. The flow mechanics involved in all ducted-fan units are illustrated in figure 8, which is a schematic sketch of the flow through a fan-in-fuselage configuration. The momentum of the free-stream air captured by the fan produces a drag force which is termed momentum drag. The line of action of this free-stream momentum is generally above the moment center of the vehicle; thus, a nose-up moment is also produced. If thrust is obtained by vectoring the fan exhaust rearward, as indicated by the example shown here, and if the line of action of this thrust force is below the center of gravity, an additional nose-up moment will be produced. These effects are illustrated in figure 9 which shows lift and drag due to the fan divided by fan static thrust, and moment due to the fan divided by the product of fan static thrust and fan radius, all plotted against free-stream velocity in knots. These data were obtained from full-scale wind-tunnel tests of the Vanguard fan-in-wing airplane and from a fan-in-fuselage configuration which utilized the General Electric lift-fan engine. These vehicles are shown in figure 10. The static disk loading for the fan-in-wing data was 12 pounds per square foot, whereas that for the fan-in-fuselage data was 215 pounds per square foot. The general characteristics anticipated from figure 8 are evident, namely, a buildup in drag and nose-up moment with speed. The indicated increase in lift with speed is due both to an increase in mass flow through the fan due to ramming of the inlet and to lift induced on the wing by the fan. It should be noted that the change of lift, drag, and moment with speed is more pronounced for the low-disk-loading configuration than it is for the high-disk-loading configuration, since a larger mass flow is required for a given thrust level.

The right-hand side of figure 9 presents the same lift, drag, and moment parameters as a function of nondimensionalized forward speed. For identical configurations this type of presentation should remove the effects of disk loading so that the differences shown here are primarily due to configuration differences. Also shown on the lift and drag plots is an estimated variation of lift and drag with speed by using simple momentum theory and assuming 100-percent inlet efficiency. As a matter of interest, the inlet loss on the fan-in-fuselage configuration was less than 5 percent of the dynamic pressure in the inlet for values of nondimensionalized speed up to 0.55. For this configuration the difference between the estimated and experimentally obtained lift was found to be due to wing lift induced by the fan. For the fan-in-wing configuration, large inlet losses were encountered at the higher nondimensionalized forward speeds, and it is believed that this fact partly accounts for the lower lift and drag obtained. The results obtained from these two investigations are remarkably similar when the effects of disk loading are eliminated by nondimensionalizing the forward speed, in spite of the large differences between the two configurations. These results indicate that the drag is largely due to momentum drag, and it is likewise believed that the pitching moment is mainly due to the change in angular momentum of the air captured by the inlet. Since these momentum effects are a function of the product of fan mass flow and flight velocity, they can be reduced by reducing the mass flow as the flight velocity is increased. One method of doing this is to transfer as much of the load as possible to the wing during transition so that the fan thrust and mass flow may be progressively reduced as the speed is increased. Also, it should be noted that the power required to overcome the momentum drag may be either large or small, depending on how much of the energy of the captured air is dissipated in losses in the system.

These momentum changes are also important for the tilting-duct designs and result in large duct normal forces and pitching moments in the transition from hovering to forward flight. These duct moments can be reduced and, in principle, could be eliminated by the use of exit vanes in the duct exhaust so that the required momentum changes are accomplished aft as well as forward of the moment center.

Also, for the tilting-duct configuration, it should be noted that good propulsive efficiencies in cruise flight must be obtained with a unit which basically is sized to meet the hovering requirement. This situation is directly analogous to that discussed previously for VTOL propellers and will require the ability to vary fan blade angle and/or duct geometry.

CONCLUSIONS

In conclusion, full-scale wind-tunnel research on various VTOL aircraft concepts conducted thus far indicate that:

1. Rotor propellers and ducted fans having sufficient blade area to support the vehicle in hovering flight will have more blade area than that required for maximum efficiency in cruise flight, regardless of disk loading. This loss in propulsive efficiency may be minimized by operating the propeller at high advance ratios. The implications of high-advance-ratio operation on efficiency, loads, and blade motions are

believed to be worthy of further study, particularly for rotor-propellers having blades free to flap, where large flapping angles have been encountered.

2. The ability of vectored-slipstream and tilt-wing aircraft to make steep descents or to decelerate is limited by the occurrence of wing stall. Continued research to eliminate or alleviate the effects of wing flow separation is believed to be desirable, particularly at large scale.

3. For ducted-fan configurations the drag and pitching moment due to the momentum changes of the air captured by the fan will possibly result in serious power and control problems in transition flight. In general, it appears desirable from both a momentum-drag and pitching-moment standpoint to carry as much lift as possible on the wing in the transition; as a result, the fan thrust output can be reduced as the flight speed is increased and thereby the associated momentum drag and moment are reduced.

Finally, as stated in the introduction, the purpose of this paper was to present the basic problem areas encountered in the various VTOL concepts tested to date. Therefore, favorable aspects of the various configurations were presumed to be outside the scope of the present discussion. Although the various problem areas discussed are believed to be of a basic nature, it is not meant to be implied that they are insurmountable but rather that further work along the lines indicated is required.

REFERENCES

1. Hickey, David H.: Full-Scale Wind-Tunnel Tests of the Longitudinal Stability and Control Characteristics of the XV-1 Convertiplane in the Autorotating Flight Range. NACA RM A55K21a, 1956.

2. Koenig, David G., Greif, Richard K., and Kelly, Mark W.: Full-Scale Wind-Tunnel Investigation of the Longitudinal Characteristics of a Tilting-Rotor Convertiplane. NASA TN D-35, 1959.

3. James, Harry A., Wingrove, Rodney C., Holzhauser, Curt A., and Drinkwater, Fred J., III: Wind-tunnel and Piloted Flight Simulator Investigation of a Deflected-Slipstream VTOL Airplane, the Ryan VZ-3RY. NASA TN D-89, 1959.

THREE VTOL TYPES

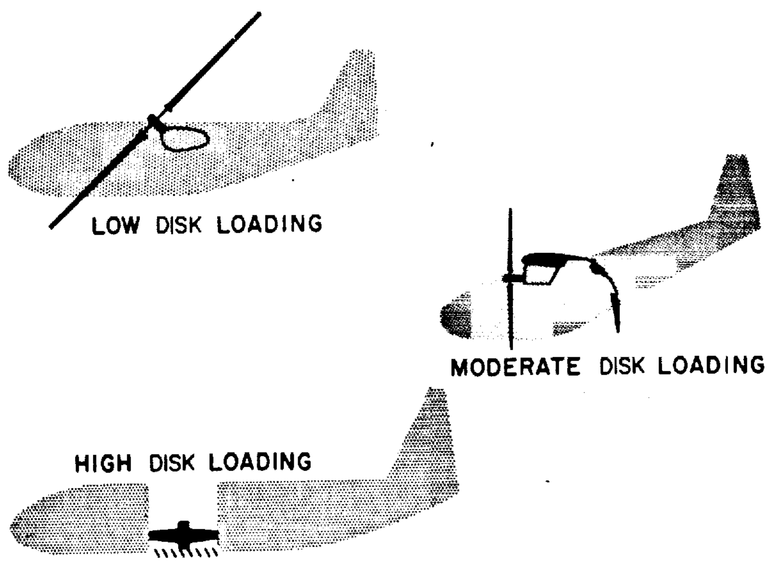

Figure 1

PROPULSIVE POWER REQUIRED VS AIRSPEED
FOR XV-I UNLOADED ROTOR CONVERTIPLANE

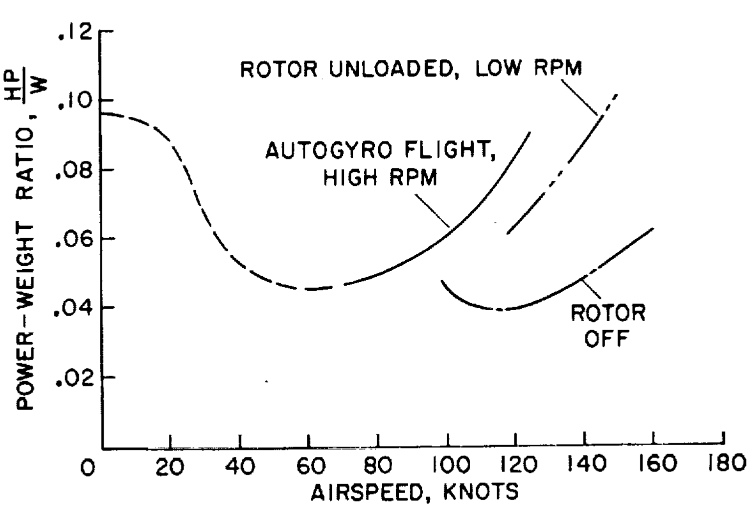

Figure 2

SHAFT POWER REQUIRED VS AIRSPEED
FOR XV-3 CONVERTIPLANE

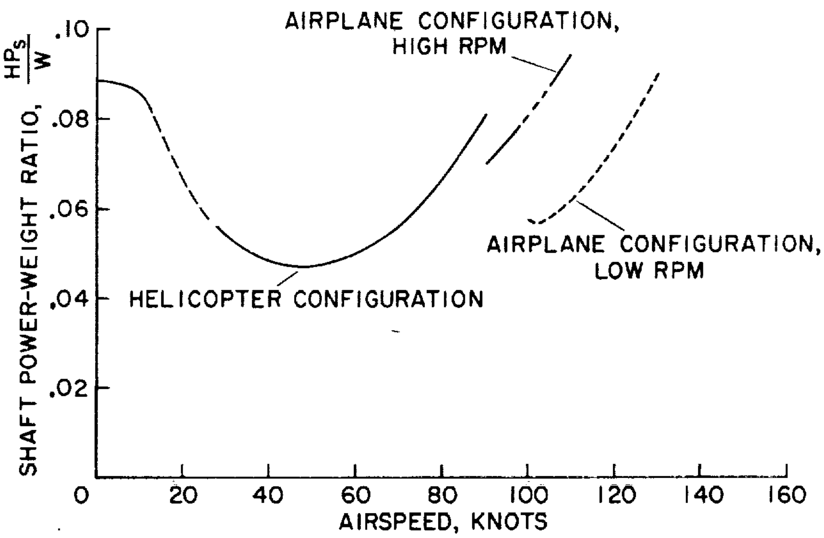

Figure 3

POWER REQUIRED AND POWER AVAILABLE
FOR XV-3 CONVERTIPLANE IN AIRPLANE FLIGHT

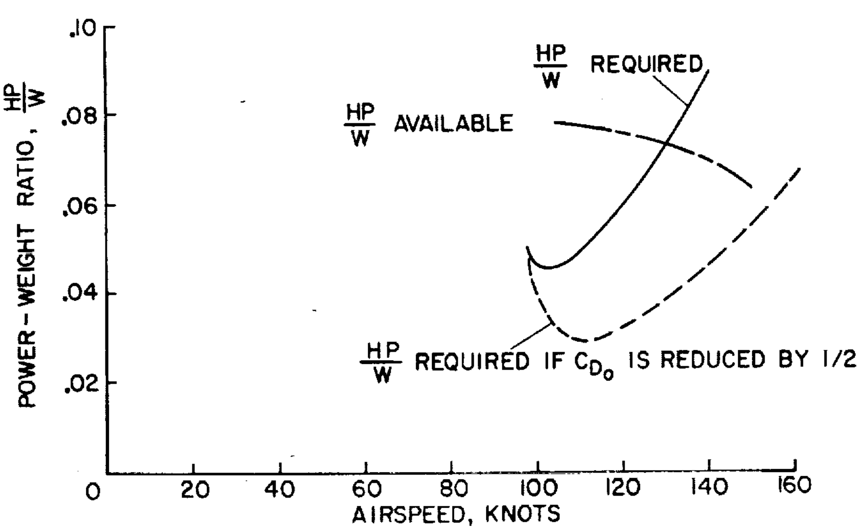

Figure 4

VARIATION OF BLADE LOADING COEFFICIENT, FOR OPTIMUM EFFICIENCY WITH ADVANCE RATIO

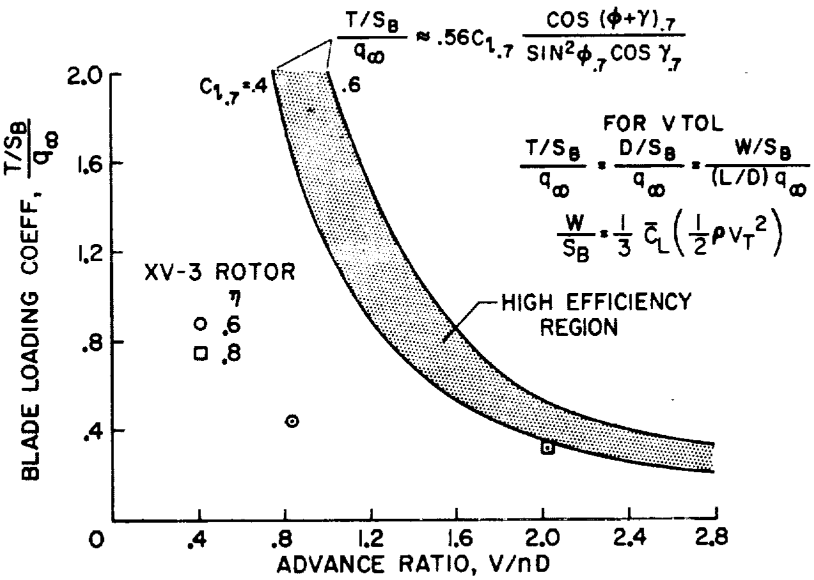

$$\frac{T/S_B}{q_\infty} \approx .56 C_{l.7} \frac{\cos(\phi+\gamma)_{.7}}{\sin^2\phi_{.7} \cos\gamma_{.7}}$$

$$\frac{T/S_B}{q_\infty} = \frac{D/S_B}{q_\infty} = \frac{W/S_B}{(L/D)\, q_\infty}$$

$$\frac{W}{S_B} = \frac{1}{3}\bar{C}_L\left(\frac{1}{2}\rho V_T^2\right)$$

Figure 5

RATIO OF DISK LOADING TO DYNAMIC PRESSURE FOR WING STALL

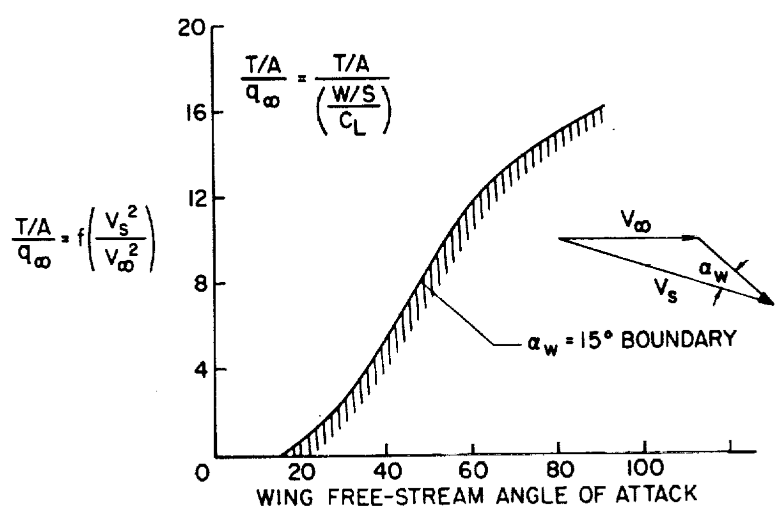

$$\frac{T/A}{q_\infty} = \frac{T/A}{\left(\frac{W/S}{C_L}\right)}$$

$$\frac{T/A}{q_\infty} = f\left(\frac{V_s^2}{V_\infty^2}\right)$$

Figure 6

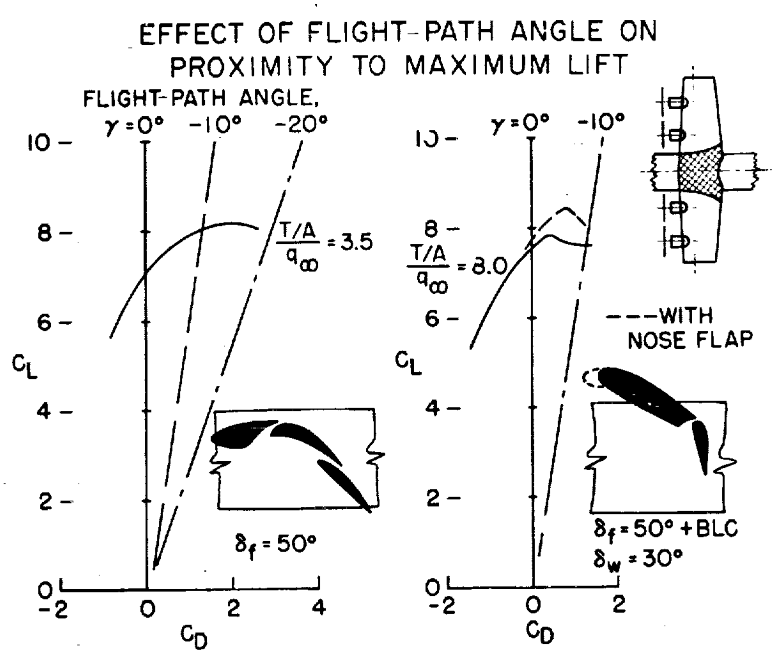

Figure 7

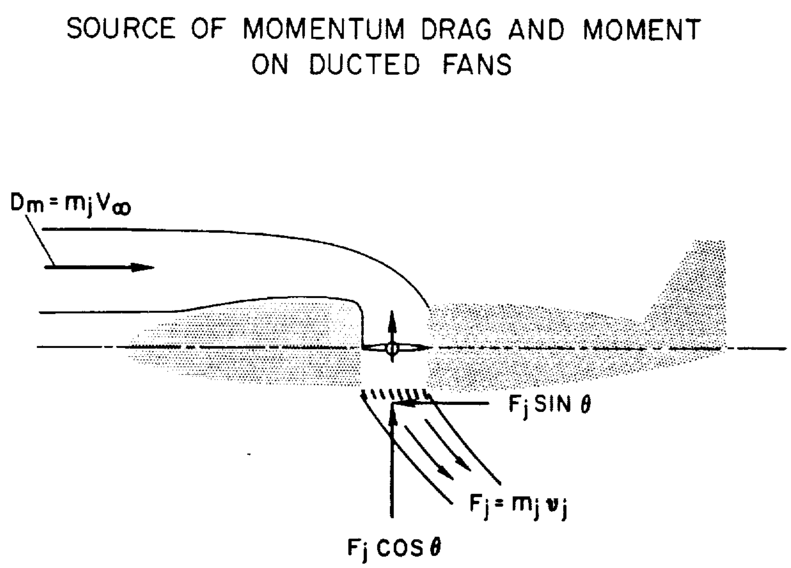

Figure 8

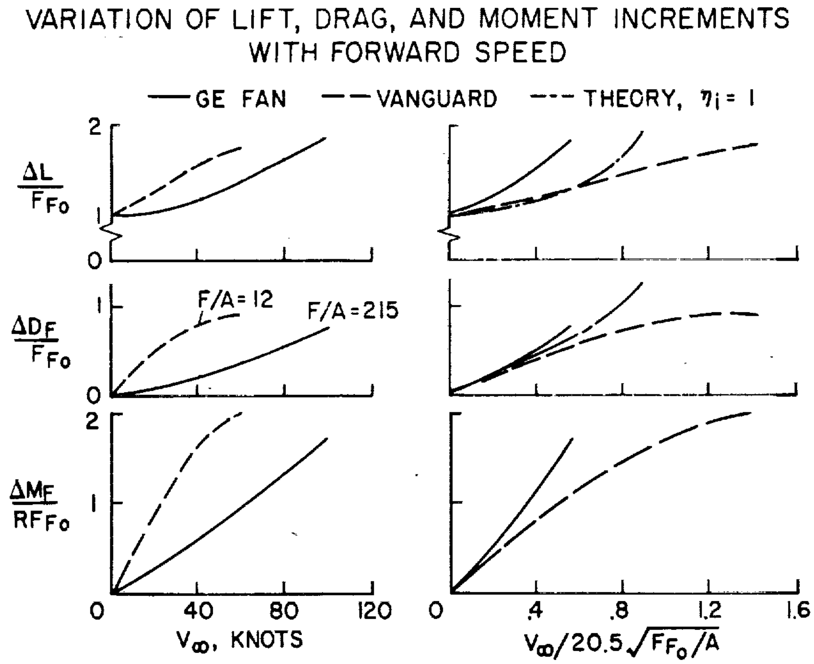

Figure 9

LIFT-FAN CONFIGURATIONS

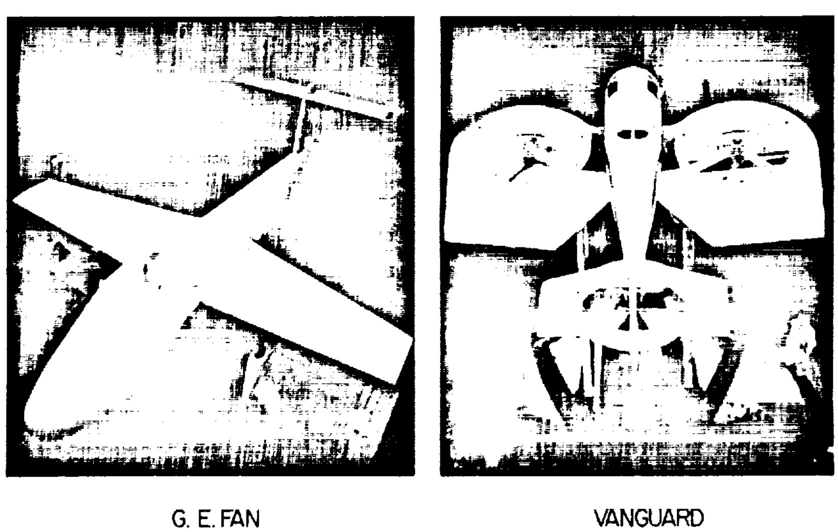

Figure 10